Nanoscale Advances

ROYAL SOCIETY OF CHEMISTRY

COMMUNICATION

View Article Online
View Journal | View Issue

Cite this: *Nanoscale Adv.*, 2022, **4**, 5009

Received 4th September 2022
Accepted 12th October 2022

DOI: 10.1039/d2na00596d

rsc.li/nanoscale-advances

Simple and sustainable synthesis of perovskite-based optoelectronic material: $CsPbBr_3$ nanocrystals *via* laser ablation in alcohol†

Simone Sansoni, Filippo M. Anoè and Moreno Meneghetti *

All-inorganic lead halide perovskite nanocrystals (NCs) have shown great potential as emerging semiconducting materials due to their excellent optoelectronic properties. However, syntheses in solution commonly use high temperatures and toxic solvents, which are obstacles for safety and sustainability of the process. In this work, laser ablation in alcohol is proposed as a simple and sustainable, ligand-free, top-down approach to synthesize $CsPbBr_3$ nanocrystals in ambient conditions. The effects of different low boiling point commercial alcohols used as solvents on the optical properties of $CsPbBr_3$ NCs colloidal solutions are investigated. Although in traditional bottom-up synthesis alcohols are usually found to be not appropriate for the synthesis of perovskite NCs, here it is demonstrated that $CsPbBr_3$ orthorhombic nanocrystals with narrow full width half maximum (FWHM < 18 nm), long photoluminescence lifetimes (up to 17.9 ns) and good photoluminescence quantum yield (PLQY up to 15.5%) can be obtained by selecting the dielectric constant and polarity of the alcohol employed for the synthesis.

Introduction

Lead halide perovskite nanocrystals (NCs) have drawn great attention in the last years and they found application in a variety of optoelectronic devices like light-emitting diodes, solar cells, transistors, laser, photo-detectors, quantum information and photocatalysis.[1–3] Such a high versatility is attributable to their plethora of desirable properties: long carrier diffusion lengths, simple bandgap tunability, high absorption coefficients and exceptional defect tolerance.[4,5] Defect tolerance is a very attractive property as it makes solution-processing a viable prospect.[6] In addition to the relatively low cost of perovskite precursor salts, the perovskite-based optoelectronics have recently gained substantial commercial appeal. However, in-vacuum "hot-injection" synthesis is the most widely used approach to produce perovskite nanocrystals, although this is a challenging approach for a sustainable process.[7] Recent approaches are based on free-amine syntheses obtained, however, at high temperature and with the usual solvents.[8] Room temperature processes, performed without environmental problems, are more attractive[9,10] and the identification of suitable green solvents is a relevant aspect to consider.[11,12] Recently, several solvents have been selected on the basis of environmental, health and safety (EHS) evaluations and guides for their selection have been created.[13] The innovative medicines initiative (IMI)-CHEM21 selection guide is used to select the solvents in the present approach.[14] Small dimension nanocrystals and colloid stability are important to get stable and high-emissive inks. In bottom-up synthesis, perovskite NCs with small dimensions are usually obtained with a shell of organic ligands, which are crucial both for colloidal stability as well as for surface defect passivation.[15–19] The low stability of lead halide perovskite NCs in such post-synthetic processes still limits their properties.[20,21] Laser ablation synthesis in solution (LASiS) has proven to be a viable top-down method for the synthesis of ligand-free lead halide perovskite NCs in ambient conditions.[22–24] In this work, LASiS process was optimized for the synthesis of all-inorganic $CsPbBr_3$ perovskite NCs in eco-sustainable solvents at ambient condition. The effects of different commercially available alcohols, used as solvent for the LASiS process, on the optical properties of $CsPbBr_3$ NCs colloidal solutions are investigated. Although in traditional bottom-up synthesis alcohols are usually found to be not beneficial for perovskite NCs,[25,26] here it is demonstrated that orthorhombic $CsPbBr_3$ nanocrystals with narrow FWHM down to 16 nm, long PL lifetimes up to 17.9 ns, and good PLQY up to 15.5% can be obtained by selecting the dielectric constant and polarity of the alcohol employed for the synthesis. The lower surface tension and higher vapor pressure of alcohols,

Department of Chemical Sciences, University of Padua, Padua 35131, Italy. E-mail: moreno.meneghetti@unipd.it

† Electronic supplementary information (ESI) available: Details of the ablation setup; $PbBr_2$ molar extinction coefficient; environmental, health and safety guidelines for solvents; optical, structural, and morphological characterization of $PbBr_2$ and $CsPbBr_3$ nanocrystals; *Z*-potential and DLS measurements of $CsPbBr_3$ nanocrystals. See DOI: https://doi.org/10.1039/d2na00596d

compared to traditional high boiling toxic solvents used for LHP processing, can be exploited in sustainable and fast compatible processing.[27,28]

Materials and methods

Materials

Lead bromide (99.999%), cesium bromide (99.999%) and all the anhydrous solvents used for the synthesis were Sigma-Aldrich products and were used without further purification.

2-Step conversion of $CsPbBr_3$ nanocrystals

Precursor solutions of $PbBr_2$ NCs were obtained by LASiS using the third harmonic of a Nd:YAG laser at 355 nm, focused on the surface of a $PbBr_2$ compressed powder round tablet with a fluence of 2 J cm^{-2}. The target was placed into a glass vial (14 mm diameter) and immersed under 4.0 ml of alcohol (see Fig. 2b). LASiS were performed for 45 min, with 9 ns laser pulses at 20 Hz repetition rate. To ensure a uniform erosion of the target, the vial was continuously moved by an automated x–y movement system, at a speed of 0.5 mm s^{-1}. The concentration of $PbBr_2$ NCs colloidal solutions, in the range of 0.5–0.7 mM, was estimated by optical extinction (see Fig. S1†). $CsPbBr_3$ NCs were produced as follows: 2.0 ml of 0.2 mM $PbBr_2$ NCs diluted solution were mixed with 50 μl of 8 mM CsBr solution in ethanol for 30 min in a sonication bath. The solutions were then centrifuged for 4 min at 5000 RCF and redispersed in the same pure alcohol to get $CsPbBr_3$ NCs colloidal solution without impurities.

1-Step *in situ* synthesis of $CsPbBr_3$ nanocrystals

100 μl of 8 mM CsBr solution in ethanol were added to 4.0 ml ablation solvent and then vigorously mixed on a vortex for 5 min before synthesis. The ablation duration, between 60 and

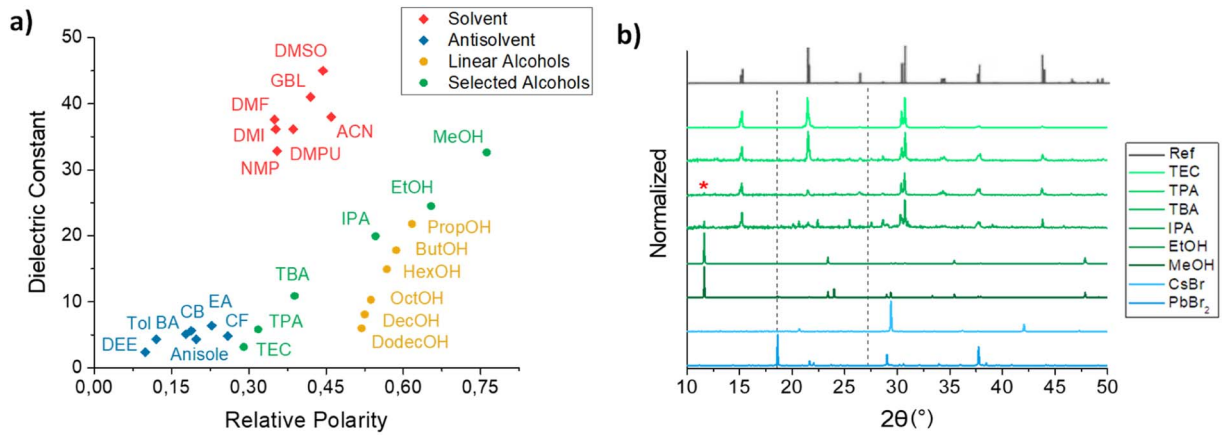

Fig. 1 (a) Dielectric constant as a function of relative polarity of most used solvents (red) and antisolvents (blue) for perovskite synthesis. It is noticeable that, contrary to linear chain alcohols (yellow), the use of branched alcohols (green) enables to reach low values of both dielectric constant and polarity. (b) XRD patterns of orthorhombic $CsPbBr_3$ perovskite NCs synthesized by LASiS in different alcohols. Contributes of non-perovskite phases at low angles are highlighted with red asterisk. Pattern of $PbBr_2$ NCs obtained by LASiS in alcohol and of CsBr powders are also reported for comparison. The orthorhombic reference spectrum (ICSD 97851) of the $CsPbBr_3$ orthorhombic phase is taken from ref. 32.

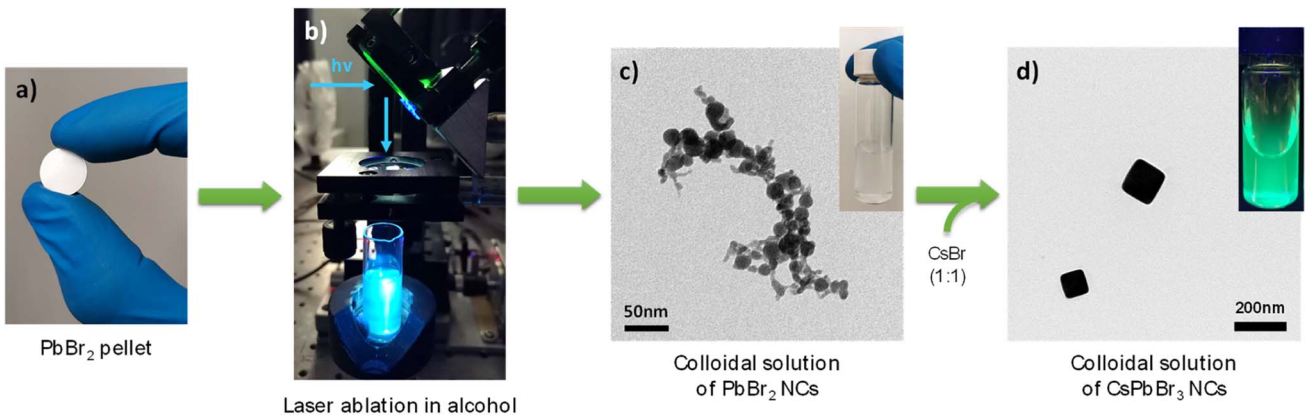

Fig. 2 Scheme of $PbBr_2$ nanocrystals synthesis by laser ablation in alcohol and their conversion into $CsPbBr_3$ colloidal solution by the 2-step protocol. (a) $PbBr_2$ compressed powder round pellet employed as target. (b) Picture of laser ablation in progress, showing the Nd:YAG laser beam focused on the surface of the target immersed in alcohol. (c) TEM image of $PbBr_2$ precursor nanocrystals; the inset shows a picture of $PbBr_2$ NCs solution under visible light. (d) TEM image of $CsPbBr_3$ perovskite nanocrystals; the inset shows a picture of $CsPbBr_3$ NCs solution under UV light.

90 min, was tuned for each sample to get a complete perovskite conversion with no unreacted CsBr in solution. All other experimental conditions/post-treatments were the same as for the "2-step conversion" samples.

Characterization

UV-visible spectra were registered with an Agilent Cary 5000 UV-Vis-NIR spectrometer using 0.2 cm quartz cuvettes. Edinburgh FLS 1000 UV/Vis/NIR photoluminescence spectrometer were employed for steady-state and time-resolved photoluminescence (SSPL and TRPL) measurements. SSPL spectra were collected exciting at 400 nm with a Xe lamp and using a PMT-850 detector. TRPL decays were registered following the time-correlated single photon counting (TCSPC) method, using a pulsed laser diode at 402.6 nm and a high-speed PMT-850 detector. Absolute PLQY were measured using an integrating sphere and exciting at 400 nm with a Xe lamp. All samples were diluted to get 0.1 Abs at the excitonic peak wavelength. TEM images were registered at 100 kV with a FEI TECNAI G2 electron microscope. XRD patterns were recorded at room temperature with a BRUKER AXS D8 ADVANCE Plus diffractometer in Bragg–Brentano geometry.

Results and discussion

EHS guidelines were followed to select the green solvents to be used for LASiS (see Fig. S2†).[14] Dielectric constant and relative polarity were considered as main parameters to evaluate the solvent- or antisolvent-like behavior towards perovskite nanocrystals.[29,30] Aliphatic alcohols were chosen as class of non-hazardous solvents. Methanol (MeOH), ethanol (EtOH), isopropanol (IPA), *tert*-butanol (TBA), *tert*-pentanol (TPA) and triethyl carbinol (TEC) were selected to investigate a wide range of dielectric constant and polarity, moving from the solvent- to antisolvent-regime (see Fig. 1a). $CsPbBr_3$ NCs were synthesized in these alcohols by following two different approaches, namely 2-step conversion and 1-step *in situ* synthesis (see Materials and methods).

$CsPbBr_3$ NCs by 2-step conversion were obtained by mixing a colloidal solution of $PbBr_2$ precursors NCs, synthesized *via*

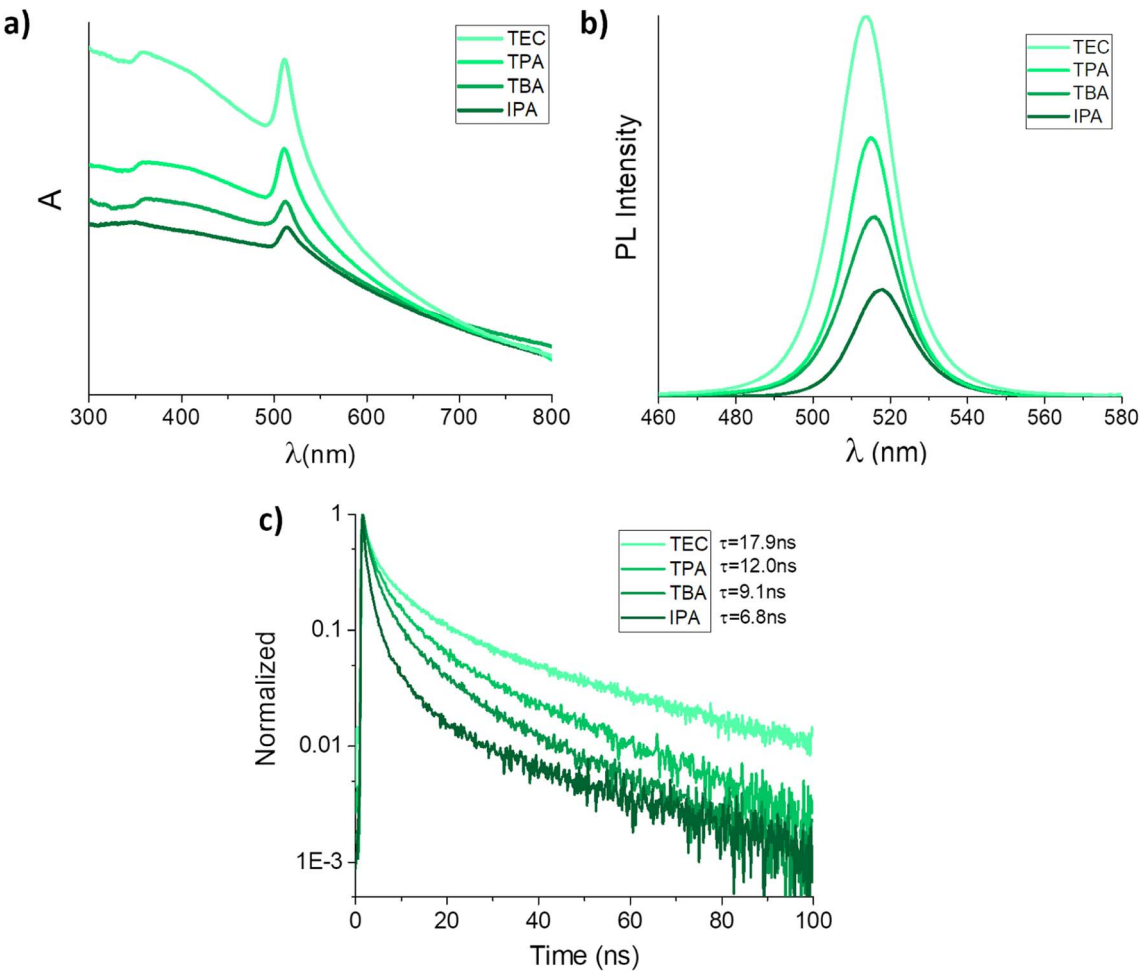

Fig. 3 Comparison of (a) UV-Vis spectra, (b) steady-state PL emissions, and (c) time-resolved PL decays of $CsPbBr_3$ NCs synthesized by 1-step *in situ* synthesis in different alcohols (PL profiles are normalized to the intensity of the respective absorption peak). The intensity-averaged lifetimes reported in (c) were calculated by three-exponential fit of the respective PL decays, following previous indications (the reported values are intensity-averaged lifetime values, see Fig. 3a).[25,35,36]

a)

SOLVENT	Abs_{MAX} (nm)	PL_{MAX} (nm)	FWHM (nm)	τ_1 (ns)	τ_2 (ns)	τ_3 (ns)	τ_{AVG} (ns)
MeOH*	--- ---	522 ---	>22 ---	0.36 ---	1.13 ---	6.09 ---	1.73 ---
EtOH	515 ---	522 ---	21 ---	0.49 ---	1.72 ---	8.81 ---	2.89 ---
IPA	514 513	521 518	20 19	0.33 0.25	1.93 2.21	9.09 12.13	5.38 6.80
TBA	513 512	519 516	18.5 17.5	0.59 0.31	2.47 3.04	10.34 16.71	7.92 9.12
TPA	511 510	517 515	18 17	0.37 0.34	2.67 3.50	12.90 19.32	10.18 12.02
TEC	510 510	515 514	16.5 16	0.42 0.31	2.74 3.55	16.25 25.22	12.64 17.94

* PL intensity quickly faded right after measurement

b)

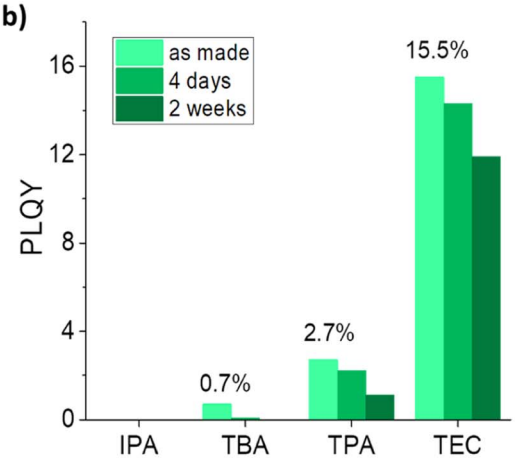

Fig. 4 (a) Table summarizing the results of optical characterizations of $CsPbBr_3$ NCs by laser ablation in alcohols. The excitonic peak positions (Abs_{MAX}) observed in UV-Vis spectra, the PL emission wavelength (PL_{MAX}) and FWHM given by SSPL measurements, and the intensity-averaged lifetime values (τ_{AVG}) calculated by three-exponential fit of the TRPL decays are listed. Data related to $CsPbBr_3$ NCs by the 2-step conversion protocol are reported with light font. (b) PLQY values measured over time for the $CsPbBr_3$ NCs by 1-step *in situ* synthesis method in different alcohols. All samples were kept in ambient conditions during aging.

laser ablation in alcohol (see Fig. S3†), with an equimolar CsBr solution in EtOH. A scheme summarizing the whole process is reported in Fig. 2 with the TEM image of the synthesized nanocrystals. The best results were obtained by exploiting the alcohols with the lowest polarity and dielectric constant among those investigated, namely TPA and TEC, getting perovskite NCs with good optical and morphological properties. The typical $CsPbBr_3$ perovskite excitonic peaks, around 515–520 nm, were observed in the UV-Vis spectra (see Fig. S4a†). Narrow and intense PL emissions were registered in SSPL measurements, while average PL lifetimes of 10.2 and 12.6 ns were estimated from TRPL decays of NCs synthesized in TPA and TEC, respectively (see Fig. S4b and c†). Cubic-shaped nanocrystals were observed by TEM analysis in both samples (see Fig. S5†), with an average size of 120–200 nm. Poor optical and morphological properties were obtained with other solvents and particularly with MeOH and EtOH, (see Fig. S4 and S5†). The XRD analysis, reported in Fig. 1b, confirmed the trend of optical and morphological properties deteriorating as the polarity of the alcohols employed for the synthesis increases.

A good crystallinity of orthorhombic $CsPbBr_3$ perovskite phases were observed for the NCs synthesized in TPA and TEC,[31,32] while unreacted precursors and Cs–Pb–Br non-perovskite phases (*e.g.*, $CsPb_2Br_5$ (ref. 33 and 34)) were found in MeOH and EtOH, with still some residuals in IPA sample. The sharp double peaks observed for example at 15.1°, 21.5° and 30.4°, show that we obtained the orthorhombic phase. The peak at low angles indicated with an asterisk is for example characteristic of the $CsPb_2Br_5$ phase.[33,34]

$CsPbBr_3$ NCs obtained by the 1-step *in situ* synthesis approach were produced during LASiS with CsBr already present in the solvent before the ablation process (see Fig. S6†). Given the poor results obtained with $CsPbBr_3$ NCs by 2-step conversion in MeOH and EtOH deriving from the different results obtained with the ablation of $PbBr_2$ (see Fig. S4a†), the 1-step *in situ* synthesis approach was used with the other alcohols. Compared to the 2-step samples synthesized in the same alcohols, the 1-step *in situ* syntheses showed important improvements of many parameters. Sharp $CsPbBr_3$ excitonic peaks were observed in the UV-Vis spectra (Fig. 3a). PL emissions significantly increased in intensity (Fig. 3b) and long average PL lifetimes were obtained from TRPL measurements, which increased up to 12.5 and 17.9 ns in the case of $CsPbBr_3$ NCs synthesized in TPA and TEC (Fig. 3c). A comparison between the optical properties of 2-step and 1-step *in situ* samples is reported in Fig. S7.†

Table in Fig. 4a summarizes all the optical characterization results of $CsPbBr_3$ NCs. Both excitonic peaks and PL emissions of the 1-step *in situ* perovskite showed a slight blueshift. This observation is in line with results obtained with smaller nanocrystals.[35,36] A more defined cubic shape of perovskite NCs was also noticed by decreasing alcohols polarity, moving from IPA to TEC, with an average size of 30–50 nm. A PLQY up to 15.5% was measured for the orthorhombic $CsPbBr_3$ NCs synthesized in TPA, showing a good quantum yield stability over several days in ambient conditions (Fig. 4b).

The PLQY and lifetime values are consistent with previous works on orthorhombic $CsPbBr_3$ nanocrystals,[32] proving the good quality of the perovskite colloids synthesized with this methodology. Despite the absence of any ligands in the $CsPbBr_3$ NCs solutions obtained by LASiS, a good colloidal stability was also observed in all samples. This is clearly related to the surface charge induced by LASiS,[37,38] which produces high z-potential values for the nanocrystals obtained by the 1-step *in situ* synthesis (see Fig. S8†) and therefore a stronger coulomb interaction among nanocrystals.

Conclusions

Laser ablation technique was used to produce colloidal solutions of all-inorganic $CsPbBr_3$ perovskite nanocrystals in commercially available branched alcohols. By selecting alcohols

with low polarity and dielectric constant it is demonstrated that, contrary to what is generally reported, orthorhombic $CsPbBr_3$ nanocrystals can be synthesized at ambient conditions in this class of eco-sustainable, low-toxic solvents. Two protocols were used for the syntheses. The first protocol, called 2-step, is based on the ablation of $PbBr_2$ and then the reaction of the obtained $PbBr_2$ nanoparticles with CsBr, whereas the second one, called 1-step, is based on the reaction of the nanoparticles with CsBr at the same time of the ablation of $PbBr_2$. It is found that the second protocol, the 1-step one, allows the synthesis of $CcPbBr_2$ with better properties. Optimized samples showed good optical and morphological properties, good crystallinity and colloidal stability, intense and narrow PL emissions (FWHM down to 16 nm), long PL lifetimes (up to 17.9 ns), and good PLQY (up to 15.5%) which was stable over many days under ambient conditions. High emissive nanocrystals with cubic symmetry[32] will be considered as a further step of this study. These results show that laser ablation in solution can be an effective alternative top-down method for the synthesis of ligand-free $CsPbBr_3$ nanocrystals in "green" solvents at ambient condition, answering the call for more sustainable production and processing of halide perovskite nanomaterials.

Conflicts of interest

The authors declare no competing financial interest.

Acknowledgements

The Edinburgh FLS 1000 UV/Vis/NIR photoluminescence spectrometer and BRUKER AXS D8 ADVANCE Plus diffractometer at the PanLab department facility were founded by the MIUR-"Dipartimenti di Eccellenza" grant NExuS. Project P-DiSC#06BIRD2020-UNIPD of the University of Padova is acknowledged for supporting the present work.

References

1 A. Dey, J. Ye, A. De, E. Debroye, S. K. Ha, E. Bladt, A. S. Kshirsagar, Z. Wang, J. Yin and Y. Wang, State of the Art and Prospects for Halide Perovskite Nanocrystals, *ACS Nano*, 2021, **15**(7), 10775–10981, DOI: **10.1021/acsnano.0c08903**.

2 C. R. Kagan, L. C. Bassett, C. B. Murray and S. M. Thompson, Colloidal Quantum Dots as Platforms for Quantum Information Science, *Chem. Rev.*, 2021, **121**, 3186–3233, DOI: **10.1021/acs.chemrev.0c00831**.

3 M. Palabathuni, S. Akhil, R. Singh and N. Mishra, Charge Transfer in Photoexcited Cesium–Lead Halide Perovskite Nanocrystals: Review of Materials and Applications, *ACS Appl. Nano Mater.*, 2022, **5**, 10097–10117.

4 J. S. Manser, J. A. Christians and P. V. Kamat, Intriguing Optoelectronic Properties of Metal Halide Perovskites, *Chem. Rev.*, 2016, **116**(21), 12956–13008, DOI: **10.1021/acs.chemrev.6b00136**.

5 M. V. Kovalenko, L. Protesescu and M. I. Bodnarchuk, Properties and Potential Optoelectronic Applications of Lead Halide Perovskite Nanocrystals, *Science*, 2017, **358**(6364), 745–750, DOI: **10.1126/science.aam7093**.

6 Y. Du, P. Liu, F. Li, X. Hou, H. Zhang, Y. Shi, S. Wang, Y. Wang, S. Guo and Q. Tai, Precursor Engineering for Performance Enhancement of Hole-Transport-Layer-Free Carbon-Based $MAPbBr_3$ Perovskite Solar Cells, *J. Alloys Compd.*, 2020, 154902, DOI: **10.1016/j.jallcom.2020.154902**.

7 J. Shamsi, A. S. Urban, M. Imran, L. De Trizio and L. Manna, Metal Halide Perovskite Nanocrystals: Synthesis, Post-Synthesis Modifications, and Their Optical Properties, *Chem. Rev.*, 2019, **119**(5), 3296–3348, DOI: **10.1021/acs.chemrev.8b00644**.

8 S. Akhil, V. G. V. Dutt and N. Mishra, Amine-Free Synthesis of Colloidal Cesium Lead Halide Perovskite Nanocrystals, *ChemNanoMat*, 2021, **7**, 342–353.

9 A. A. M. Brown, B. Damodaran, L. Jiang, J. N. Tey, S. H. Pu, N. Mathews and S. G. Mhaisalkar, Lead Halide Perovskite Nanocrystals : Room Temperature Syntheses toward Commercial Viability, *Adv. Energy Mater.*, 2020, **2001349**, 1–19, DOI: **10.1002/aenm.202001349**.

10 A. A. M. Brown, P. Vashishtha, T. J. N. Hooper, Y. F. Ng, G. V. Nutan, Y. Fang, D. Giovanni, J. N. Tey, L. Jiang and B. Damodaran, Precise Control of $CsPbBr_3$ Perovskite Nanocrystal Growth at Room Temperature: Size Tunability and Synthetic Insights, *Chem. Mater.*, 2021, **33**, 2387–2397, DOI: **10.1021/acs.chemmater.0c04569**.

11 M. Zhang, D. Xin, X. Zheng, Q. Chen and W. H. Zhang, Toward Greener Solution Processing of Perovskite Solar Cells, *ACS Sustainable Chem. Eng.*, 2020, **8**(35), 13126–13138, DOI: **10.1021/acssuschemeng.0c04289**.

12 R. Vidal, J. A. Alberola-Borràs, S. N. Habisreutinger, J. L. Gimeno-Molina, D. T. Moore, T. H. Schloemer, I. Mora-Seró, J. J. Berry and J. M. Luther, Assessing Health and Environmental Impacts of Solvents for Producing Perovskite Solar Cells, *Nature Sustainability*, 2021, **4**(3), 277–285, DOI: **10.1038/s41893-020-00645-8**.

13 C. J. Clarke, W. C. Tu, O. Levers, A. Bröhl and J. P. Hallett, Green and Sustainable Solvents in Chemical Processes, *Chem. Rev.*, 2018, **118**(2), 747–800, DOI: **10.1021/acs.chemrev.7b00571**.

14 D. Prat, A. Wells, J. Hayler, H. Sneddon, C. R. McElroy, S. Abou-Shehada and P. J. Dunn, CHEM21 Selection Guide of Classical- and Less Classical-Solvents, *Green Chem.*, 2016, **18**(1), 288–296, DOI: **10.1039/c5gc01008j**.

15 S. R. Smock, T. J. Williams and R. L. Brutchey, Quantifying the Thermodynamics of Ligand Binding to $CsPbBr_3$ Quantum Dots, *Angew. Chem., Int. Ed.*, 2018, **57**(36), 11711–11715, DOI: **10.1002/ANIE.201806916**.

16 B. Chen, P. N. Rudd, S. Yang, Y. Yuan and J. Huang, Imperfections and Their Passivation in Halide Perovskite Solar Cells, *Chem. Soc. Rev.*, 2019, **48**, 3842, DOI: **10.1039/c8cs00853a**.

17 Y. Yang, H. Qin, M. Jiang, L. Lin, T. Fu, X. Dai, Z. Zhang, Y. Niu, H. Cao and Y. Jin, Entropic Ligands for Nanocrystals: From Unexpected Solution Properties to Outstanding Processability, *Nano Lett.*, 2016, **16**, 2127–2132, DOI: **10.1021/acs.nanolett.6b00737**.

18 L. M. Wheeler, E. M. Sanehira, A. R. Marshall, P. Schulz, M. Suri, N. C. Anderson, A. Christians, D. Nordlund, D. Sokaras and T. Kroll, Targeted Ligand-Exchange Chemistry on Cesium Lead Halide Perovskite Quantum Dots for High-Efficiency Photovoltaics, *J. Am. Chem. Soc.*, 2018, **140**, 10504–10513, DOI: **10.1021/jacs.8b04984**.

19 J. Yuan, C. Bi, S. Wang, R. Guo, T. Shen, L. Zhang and J. Tian, Spray-Coated Colloidal Perovskite Quantum Dot Films for Highly Efficient Solar Cells, *Adv. Funct. Mater.*, 2019, **1906615**, 1–7, DOI: **10.1002/adfm.201906615**.

20 K. Hills-Kimball, H. Yang, T. Cai, J. Wang and O. Chen, Recent Advances in Ligand Design and Engineering in Lead Halide Perovskite Nanocrystals, *Adv. Sci.*, 2021, **8**, 2100214–2100258, DOI: **10.1002/advs.202100214**.

21 S. Cho, J. Kim, S. M. Jeong, M. J. Ko, J.-S. Lee and Y. Kim, High-Voltage and Green-Emitting Perovskite Quantum Dot Solar Cells via Solvent Miscibility-Induced Solid-State Ligand Exchange, *Chem. Mater.*, 2020, **32**, 8808–8818, DOI: **10.1021/acs.chemmater.0c02102**.

22 F. Lamberti, L. Litti, M. De Bastiani, R. Sorrentino, M. Gandini, M. Meneghetti and A. Petrozza, High-Quality, Ligands-Free, Mixed-Halide Perovskite Nanocrystals Inks for Optoelectronic Applications, *Adv. Energy Mater.*, 2017, 1601703–1601707, DOI: **10.1002/aenm.201601703**.

23 A. Rizzo, F. Lamberti, M. Buonomo, N. Wrachien, L. Torto, N. Lago, S. Sansoni, R. Pilot, M. Prato and N. Michieli, Understanding Lead Iodide Perovskite Hysteresis and Degradation Causes by Extensive Electrical Characterization, *Sol. Energy Mater. Sol. Cells*, 2019, **189**, 43–52, DOI: **10.1016/j.solmat.2018.09.021**.

24 S. Sansoni, M. De Bastiani, E. Aydin, E. Ugur, F. H. Isikgor, A. Al-Zahrani, F. Lamberti, F. Laquai, M. Meneghetti and S. De Wolf, Eco-Friendly Spray Deposition of Perovskite Films on Macroscale Textured Surfaces, *Adv. Mater. Technol.*, 2020, **5**(2), 1901009–1901014, DOI: **10.1002/admt.201901009**.

25 A. Zhao, Y. Sheng, C. Liu, S. Yuan, X. Shan, Y. Di and Z. Gan, Fluorescent Dynamics of $CsPbBr_3$ Nanocrystals in Polar Solvents: A Potential Sensor for Polarity, *Nanotechnology*, 2021, **32**(13), 135701, DOI: **10.1088/1361-6528/abd2e9**.

26 L. Rao, Y. Tang, C. Song, K. Xu, E. T. Vickers, S. Bonabi Naghadeh, X. Ding, Z. Li and J. Z. Zhang, Polar-Solvent-Free Synthesis of Highly Photoluminescent and Stable $CsPbBr_3$ Nanocrystals with Controlled Shape and Size by Ultrasonication, *Chem. Mater.*, 2019, **31**(2), 365–375, DOI: **10.1021/acs.chemmater.8b03298**.

27 Y. Deng, C. H. van Brackle, X. Dai, J. Zhao, B. Chen and J. Huang, Tailoring Solvent Coordination for High-Speed, Room-Temperature Blading of Perovskite Photovoltaic Films, *Sci. Adv.*, 2019, **5**(12), 1–9, DOI: **10.1126/sciadv.aax7537**.

28 Y. Y. Kim and J. Seo, Roll-to-Roll Gravure-Printed Flexible Perovskite Solar Cells Using Eco-Friendly Antisolvent Bathing with Wide Processing Window, *Nat. Commun.*, 2020, **11**, 5146–5156, DOI: **10.1038/s41467-020-18940-5**.

29 T. Bu, L. Wu, X. Liu, X. Yang, P. Zhou, X. Yu, T. Qin, J. Shi, S. Wang and S. Li, Synergic Interface Optimization with Green Solvent Engineering in Mixed Perovskite Solar Cells, *Adv. Energy Mater.*, 2017, **7**(20), 1–10, DOI: **10.1002/aenm.201700576**.

30 Y. Li, H. Huang, Y. Xiong, A. F. Richter, S. V. Kershaw, J. Feldmann and A. L. Rogach, Using Polar Alcohols for the Direct Synthesis of Cesium Lead Halide Perovskite Nanorods with Anisotropic Emission, *ACS Nano*, 2019, **13**(7), 8237–8245, DOI: **10.1021/acsnano.9b03508**.

31 S. Sun, D. Yuan, Y. Xu, A. Wang and Z. Deng, Ligand-Mediated Synthesis of Shape-Controlled Cesium Lead Halide Perovskite Nanocrystals via Reprecipitation Process at Room Temperature, *ACS Nano*, 2016, **10**(3), 3648–3657, DOI: **10.1021/acsnano.5b08193**.

32 L. Wang, K. Fu, R. Sun, H. Lian, X. Hu and Y. Zhang, Ultra-Stable $CsPbBr_3$ Perovskite Nanosheets for X-Ray Imaging Screen, *Nano-Micro Lett.*, 2019, **11**(52), DOI: **10.1007/s40820-019-0283-z**.

33 J. Feng, X. Han, H. Huang, Q. Meng, Z. Zhu, T. Yu, Z. Li and Z. Zou, Curing the Fundamental Issue of Impurity Phases in Two-Step Solution-Processed $CsPbBr_3$ Perovskite Films, *Sci. Bull.*, 2020, **65**(9), 726–737, DOI: **10.1016/j.scib.2020.01.025**.

34 L. Nasi, D. Calestani, F. Mezzadri, F. Mariano, A. Listorti, P. Ferro, M. Mazzeo and R. Mosca, All-Inorganic $CsPbBr_3$ Perovskite Films Prepared by Single Source Thermal Ablation, *Front. Chem.*, 2020, **8**, 1–10, DOI: **10.3389/fchem.2020.00313**.

35 J. Chen, C. Zhang, X. Liu, L. Peng, J. Lin and X. Chen, Carrier Dynamic Process in All-Inorganic Halide Perovskites Explored by Photoluminescence Spectra, *Photonics Res.*, 2021, **9**(2), 020151–020170, DOI: **10.1364/prj.410290**.

36 I. Lignos, R. M. MacEiczyk, M. V. Kovalenko and S. Stavrakis, Tracking the Fluorescence Lifetimes of Cesium Lead Halide Perovskite Nanocrystals during Their Synthesis Using a Fully Automated Optofluidic Platform, *Chem. Mater.*, 2020, **32**(1), 27–37, DOI: **10.1021/acs.chemmater.9b03438**.

37 D. Zhang, B. Gökce and S. Barcikowski, Laser Synthesis and Processing of Colloids: Fundamentals and Applications, *Chem. Rev.*, 2017, **117**(5), 3990–4103, DOI: **10.1021/acs.chemrev.6b00468**.

38 H. Zeng, X. W. Du, S. C. Singh, S. A. Kulinich, S. Yang, J. He and W. Cai, Nanomaterials via Laser Ablation/Irradiation in Liquid: A Review, *Adv. Funct. Mater.*, 2012, **22**(7), 1333–1353, DOI: **10.1002/adfm.201102295**.